The Scientific Journal of King Faisal University

Basic and Applied Sciences

Ultra-Short Pulses Generation of Free Electron Laser

Thair Abdulkareem Khalil Al-Aish[1] and Hanady Amjed Kamil[2]

[1] Department of Physics, College of Education for Pure Sciences Ibn Al-Haitham, University of Baghdad, Baghdad, Iraq
[2] Directorate of Education of First Karkh, Ministry of Education, Baghdad, Iraq

LINK	RECEIVED	ACCEPTED	PUBLISHED ONLINE	ASSIGNED TO AN ISSUE
https://doi.org/10.37575/b/sci/220045	06/10/2022	01/12/2022	01/12/2022	01/12/2022
NO. OF WORDS	NO. OF PAGES	YEAR	VOLUME	ISSUE
3643	5	2022	23	2

ABSTRACT

The major problem facing the development of civil and military laser applications lies in the attempts to obtain short pulses close to the length of the bond that connects the atoms of certain materials. In this paper, an executable program has been constructed to simulate and analyze the generation of ultra-short free electron laser pulses; it contains several parameters directing the creation of short pulses within a time duration of femtoseconds (fs). On analyzing the simulation results, it can be concluded that it is possible to generate ultra-short pulses with a duration of about 7.4 – 87.4 fs with the storage ring free-electron laser Fabry–Perot resonator with noticeably short wavelengths (11.4–190.2) for the output laser beam.

KEYWORDS

Homogenous broadening; SR-FEL; undulator; energy spread gain; Q- switching

CITATION

Al-Aish, T.A.K. and Kamil, H.A. (2022). Ultra-short pulses generation of free electron laser. *The Scientific Journal of King Faisal University: Basic and Applied Sciences*, **23**(2), 28–32. DOI: 10.37575/b/sci/220045

1. Introduction

The number of laser applications is constantly increasing in the civil and military fields due to the generation of very short-wavelength laser beams. The fields in which these are used include nonlinear optics, the spectroscopy of materials, medical treatment, the destruction of military targets, plasma remote sensing, high-speed photography, space, and astronomy (Haarlammert and Zacharias, 2009; Kamil and Al-Aish, 2022; Al-Aish and Jawad, 2017; Benson *et al.*, 2011; Varro, 2012).

Conventional laser oscillators have been used to create these ultra-short pulses primarily using the mode-locked oscillation technique. The pulse generated by this technique has a duration roughly the inverse of the gain width. One of the first successful attempts to generate ultrashort pulses was in 1986, using Ti:Sapphire as a preferred gain medium with good beam quality and high output power (Moulton, 1986).

However, due to the short bandwidth of the pulses, this technique has fallen short of producing a series of short pulses in less than a picosecond. Nonetheless, the gain spectrum width of a free electron laser (FEL) is essentially very wide in contrast to that of most conventional lasers, thus enabling a FEL to create ultra-short pulses. The storage ring free-electron laser (SR-FEL) is a self-mode locked optical system and represents a technique to produce a shorter-wavelength beam laser (Varro, 2012; Hannon, 2008; Mahmood and Al-Aish, 2020; Al-Aish, 2017; Kamil *et al.*, 2019).

In this paper, the undulator parameters have been altered to produce short pulses at a femtosecond time duration with the Fabry–Perot resonator. In contrast, the optical pulses of an SR-FEL are several picoseconds, full width at half maximum.

2. The Technique and Implementation of the Work

The ability of energy spread sources to prompt additional gain broadening, homogeneously and non-homogeneously, should be considered when designing a Fabry–Perot resonator for the FEL gain medium. This will simultaneously lead to an increase in longitudinal modes, besides those already present within the gain profile in the ultra-short wavelength region, mainly owing to long cavity length. These broadening effects significantly influence the small signal gain and saturation intensity. The homogenous broadening $\left(\frac{\Delta\omega}{\omega}\right)_{hom}$ (as a gain spectrum) is related to L_u (the length of the undulator) and N_u (the number of electron wavelengths), which can be written as

$$\left(\frac{\Delta\omega}{\omega}\right)_{hom} = \frac{1}{2}\,N_u \tag{1}$$

where ω is the angular frequency.

The number N_u is given by the equation below (Al-Aish and Kamil, 2022; Parvin *et al.*, 1997; Mehravaran and Dorranian, 2010; Kawamura *et al.*, 1987):

$$N_u = \frac{L_u}{\lambda_u} \tag{2}$$

where L_u is the length of the undulator and λ_u is the wavelength of an electron.

The nonhomogeneous broadening is due to energy spread $\in_s$ of the electron beam and emittance $\in_i$ $(i = x + y)$ as follows (Parvin *et al.*, 2012):

$$\in_s = 4\,\sigma\,N_u \tag{3}$$

where σ is the natural root-mean-square energy spread with values ranging from 0.001-0.0001.

Fine alteration of pulse duration can be conducted by adjusting the energy emittance $\in_i$ of the storage ring, such that equal to zero is in correspondence with fs duration and $\in_s$ equal to one is attributed to the picosecond pulse length.

The emittance of the $\in_i$ electron beam is one of the critical factors concerning the storage ring for FEL operations. At relatively small values of energy spread, the total broadening $\left(\frac{\Delta\omega}{\omega}\right)_{total}$ in an FEL for both homogenous and nonhomogeneous effects can be written as (Parvin *et al.*, 2012; Dattoli *et al.*, 1993).

$$\left(\frac{\Delta\omega}{\omega}\right)_{total} = \left(\frac{\Delta\omega}{\omega}\right)_{hom}\sqrt{1+\in_i^2+\in_s^2} \tag{4}$$

The gain broadening corresponds to a greater number of longitudinal modes, leading to shorter pulses and a significant reduction in the output intensity. Absorption losses in SR-FEL are the main reason

Corresponding Author: Thair Abdulkareem Khalil Al-Aish 009647801693969, thair.ak.i@ihcoedu.uobaghdad.edu.iq

behind power growth and gain reduction. A small signal gain and corresponding losses of the resonator are the basis of the FEL system.

The primary purpose of technology is to create a laser beam that has high power with exceedingly small $\in_s$, broadening, and $\in_i$. The generation of pulses of femtosecond duration, where one or sometimes several pulses are circulating in the laser resonator, is mainly achieved through the mode-locking technique. For passive Q switching (self-Q switching), the losses are automatically modulated with a saturable absorber. Modulation is responsible for the loss in the resonator, which arises from the radiative damping of electron energy in the undulator (Penzkofer, 1988).

The round-trip time τ_r of the resonator is equal to the inverse value of the free spectral range (FSR) of the resonator (see Figure 1), which is given by the equation (Parvin *et al.*, 2012; Dattoli *et al.*, 1993; Penzkofer, 1988; Davis, 1996).

$$\tau_r = \frac{1}{FSR} = \frac{2L}{c} \tag{5}$$

where L is the length of the Fabry–Perot resonator and c is the velocity of light.

The number of the n_{mode} is given by

$$n_{mode} = \Delta v_{gain}\, \tau_r \tag{6}$$

where Δv_{gain} is the gain bandwidth. The duration of the mode-locked pulses τ can be written in the following equation:

$$\tau = \frac{\tau_r}{n_{mode}} = \frac{1}{\Delta v_{gain}} \tag{7}$$

Figure 1: The round-trip time duration of the mode-locked pulses.

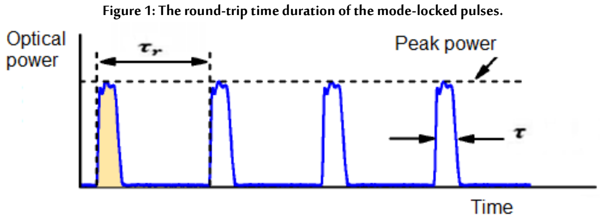

The homogenous broadening $\left(\frac{\Delta\omega}{\omega}\right)_{hom}$, depends on the number of undulator periods N_u in the half-maximum full width, and can be written in the following equation:

$$\Delta\omega_{hom} = \frac{2\pi c}{\lambda\, N_u} \tag{8}$$

where λ is the wavelength of the output laser.

$$\lambda = \frac{\lambda_u}{2\gamma^2}\left(1 + \frac{k^2}{2}\right) \tag{9}$$

$$\gamma = \frac{E_e}{m_e c^2} \tag{10}$$

$$k = \frac{e\,\beta\,\lambda_u}{2\pi\, m_e c} \tag{11}$$

where γ is the relativistic Lorentz factor, E_e the electron beam energy, m_e the electron mass, β the magnetic field, and k the undulator parameter (Dhedan *et al.*, 2022; Ali *et al.*, b2022; Al-Aish *et al.*, 2019).

The FEL comprises four main parts (electron gun, linear accelerator, undulator, and Fabry–Perot resonator), as shown in Figure 2.

Figure 2: The four main parts of the FEL.

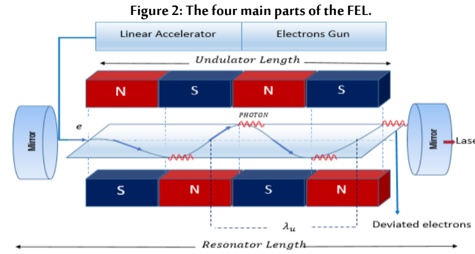

The reflection of the output mirror R is given below (Davis, 1996):

$$R = 1 - A - T \tag{12}$$

where A is the absorption loss and T the transmittance of the output mirror. It can be calculated by (Parvin *et al.*, 2012):

$$T = \frac{AR[g_0 L + \ln R]}{1 - R} \tag{13}$$

where g_0 is the small signal gain per unit length, written by the equation emittance ($\in_i$ $(i = x + y) \approx 0$) (Parvin *et al.*, 2012; Dattoli *et al.*, 1993; Penzkofer, 1988; Davis, 1996; Dhedan *et al.*, 2022):

$$g_0 = \frac{16\pi\, k^2\, N_u\, I}{\lambda_u\, I_0 \gamma \left(\sqrt{1 + \in_s^2}\right)(1 + k^2)} \tag{14}$$

where I is the current of the electron beam.

The gain and gain factor in the stimulated emission process is considered small, so it is necessary to reduce all the causes of loss in the laser device, including the loss caused by its absorption by the resonator mirrors. Mirrors for the SR-FEL in ultrashort wavelength must have high reflectivity and resistance against coherent photons.

Many layers of dielectric coatings with high reflectivity are used to coat the mirrors instead of metallic coatings (such as aluminum oxide, hafnium oxide, and hybrid systems combining fluoride and oxide materials) since dielectric coatings do not absorb light, and nearly 100% of the incident light becomes reflective without any loss.

These successive layers of thickness (t) are $\lambda/4$, and successive refractive indexes (high then low, as shown in Figure 3) are successively deposited on the glass substrate. Because of the difference in the phase that occurs at the point of contact of any two layers, all the reflected rays are in one phase and interfere constructively. Usually, more than twenty layers are used to obtain a reflectivity of approximately 99.9% (Wieduwilt *et al.*, 2014; Zegadi *et al.*, 2022).

Figure 3: Successive refractive indexes (high, then low).

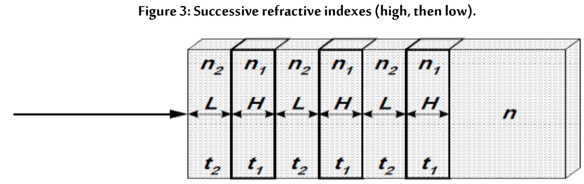

The reflectivity of the reflected light in the case of a multi-layered mirror is calculated as follows:

$$R = \frac{n_2^{q+1} - n\, n_1^{q-1}}{n_2^{q+1} - n\, n_1^{q+1}} \tag{15}$$

where n is the refractive index of the substrate, n_1 the high dielectric layer refractive index, n_2 the low dielectric layer refractive index, and q the number of layers.

While the reflectivity of the metal mirror is dependent on the density of metal ρ (g/cm3) and the wavelength λ (in micrometer) of the laser used, reflectivity is as follows:

$$R = 100 - 3.65\sqrt{\frac{\rho}{\lambda}} \tag{16}$$

The mode-locked pulse duration τ following a Lorentzian distribution, is given by the equation (Parvin *et al.*, 2012; Dattoli *et al.*, 1993; Penzkofer, 1988; Davis, 1996; Kawamura *et al.*, 1987):

$$\tau = \frac{2.773}{\sqrt{1+\epsilon_s^2}}\left(\frac{\lambda\, L_u}{c\, \lambda_u}\right) \tag{17}$$

In the SR-FEL resonator, the pulses are equal to the round-trip time τ_r. This achieves the gain switching necessary to produce a series of pulses, which requires a suitable gain broadening. When the bunching frequency v is tuned to the FSR, the repetition time of the pulse becomes equal to τ_r.

$$v = FSR = \frac{1}{\tau_r} = \frac{C}{2L} \tag{18}$$

3. Results and discussion of the simulation

An executable program was constructed using Matlab 2019 software (as shown in Figure 4) to simulate and analyze the generation of shorter pulses of FEL. It contained several parameters to produce shorter pulses of femtosecond duration.

Figure 4: The implementation of an executable program to produce shorter pulses in fs duration and summary of the values of the optimum parameters for the FEL.

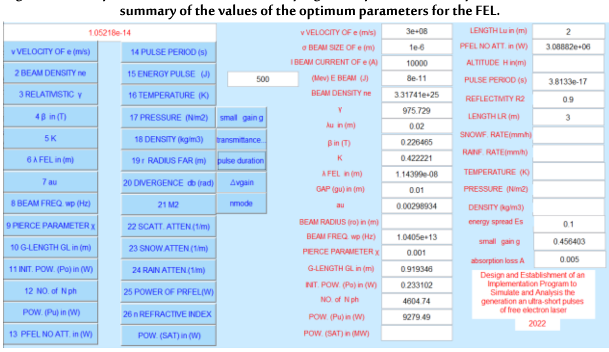

Table 1 shows the results of the simulation for the relation between the energy spread ϵ_s vs. the small signal gain g_0 and transmittance T when the wavelength of the electron $\lambda_u$is equal to 0.02, 0.03, and 0.04.

Table 1: The results of simulation for ϵ_s vs g_0 and T.

ϵ_s	$\lambda_u = 0.02$ $\lambda = 11.4\,nm$ $k = 0.422221$		$\lambda_u = 0.03$ $\lambda = 42.11\,nm$ $k = 0.654025$		$\lambda_u = 0.04$ $\lambda = 190.2\,nm$ $k = 4.01353$	
	g_0	T	g_0	T	g_0	T
0.1	0.456403	0.0568732	3.80327	0.5087	10.2715	1.38191
0.2	0.449776	0.0559785	3.74810	0.501252	10.1229	1.36185
0.3	0.439345	0.0545704	3.66124	0.489526	9.88896	1.33027
0.4	0.425890	0.0527539	3.54921	0.474402	9.58717	1.28953
0.5	0.410280	0.0506466	3.41923	0.456855	9.23696	1.24225
0.6	0.393347	0.0483606	3.27821	0.437817	8.85696	1.19095
0.7	0.375805	0.0459925	3.13212	0.418095	8.46318	1.13779
0.8	0.358215	0.0436178	2.98562	0.398317	8.06822	1.08447
0.9	0.340986	0.0412919	2.84211	0.378944	7.68124	1.03223
1	0.324392	0.0390517	2.70389	0.360284	7.30844	0.981898

Figure 5-a shows the effect of changing the energy spread ϵ_s on the small signal gain g_0, which has an inverse relationship according to equation 14. A decrease in the value of the small signal gain g_0 due to increasing values of the energy spread ϵ_s is noted. This effect becomes more evident at high values of the electron wavelengthλ_u. This is due to a decrease in the number N_u values according to equation 2 and a decrease in the homogenous broadening $\left(\frac{\Delta\omega}{\omega}\right)_{hom}$ according to equation 8. All these decrease the average number of coherent photons resulting from the passage of accelerated electrons through the β magnetic field.

Table 1 shows an increase in the value of the wavelength of the electronλ_u as a result of an increase in the wavelength values of the output laser λ and k according to equations 9 and 11. It is also noted that at the short wavelength of the resulting laser beam (λ = 11.4 nm), the gain $g_0$is smaller compared to that at a longer wavelength (λ = 190.2 nm).

Figure 5-b shows the effect of changing the energy spread ϵ_s on the transmittance T. Where the relation is inverse according to equations 13 and14, a decrease in the value of the transmittance T due to an increase in the energy spread $\epsilon_s$value is noted. The effect is more evident at higher values of electron wavelength λ_u, resulting from an increase in the gain values, and thus the transmittance T according to equation 13.

Tables 2, 3, and 4 show the results of the simulation for the relation between the energy spread ϵ_s vs. the mode-locked pulse duration τ, the gain bandwidth Δv_{gain},and the number of n_{mode} when the wavelength of the electron $\lambda_u$is equal to 0.02, 0.03, and 0.04.4.

Table 1: The simulation results for ∈s vs. τ ∆vgain and nmode when λu = 0.02 m.

ϵ_s	$\lambda_u = 0.02$m	$\tau_r = 20ns$	$L = 3$m
	$\tau(fs)$	$\Delta v_{gain} s^{-1}T$	n_{mode} M
0.1	10.5218	95.0407	1.9008
0.2	10.3689	96.4419	1.9288
0.3	10.1283	98.733	1.9746
0.4	9.81797	101.854	2.0370
0.5	9.45792	105.731	2.1146
0.6	9.06737	110.286	2.2057
0.7	8.66279	115.436	2.3087
0.8	8.25713	121.108	2.4221
0.9	7.85980	127.230	2.5445
1	7.47715	133.741	2.6748

Table 2: The simulation results for ∈s vs. τ∆vgain and nmode when λu = 0.03 m.

ϵ_s	$\lambda_u = 0.03$m	$\tau_r = 20ns$	$L = 3$m
	$\tau(fs)$	$\Delta v_{gain} s^{-1}T$	n_{mode} M
0.1	25.8203	38.7292	0.7745
0.2	25.4452	39.3001	0.7860
0.3	24.8547	40.2338	0.8046
0.4	24.0932	41.5056	0.8301
0.5	23.2096	43.0856	0.8617
0.6	22.2512	44.9414	0.8988
0.7	21.2583	47.0403	0.9408
0.8	20.2629	49.3514	0.9870
0.9	19.2878	51.8462	1.0369
1	18.3488	54.4995	1.0899

Table 3: The simulation results for ∈s vs. τ∆vgain and nmode when λu = 0.04 m.

ϵ_s	$\lambda_u = 0.04$m	$\tau_r = 20ns$	$L = 3$m
	$\tau(fs)$	$\Delta v_{gain} s^{-1}T$	n_{mode} M
0.1	87.4701	11.4325	0. 2286
0.2	86.1993	11.601	0.2320
0.3	84.1991	11.8766	0.2375
0.4	81.6191	12.252	0.2450
0.5	78.6259	12.7185	0.2543
0.6	75.3791	13.2663	0.2653
0.7	72.0157	13.8859	0.2777
0.8	68.6434	14.568	0.2913
0.9	65.3403	15.3045	0.3060
1	62.1592	16.0877	0.3217

Figure 5-c shows the effect of changing the energy spread ϵ_s on the pulse duration τ. Where the relation is inverse according to equation 17, there is a decrease in the value of the pulse duration τ as a result of an increase in the energy spread ϵ_s value. The effect is more evident at high values of the electron wavelength λ_u, where short pulses between $\tau = 7.47715\, fs$ and $\tau = 87.4701\, fs$ are generated by the Fabry–Perot resonator.

Figure 5-d and Figure 5-e show the effect of changing the energy spread ϵ_s on the gain bandwidth Δv_{gain} and the number of n_{mode} when the wavelength of the electron $\lambda_u$is equal to 0.02, 0.03, and 0.04. Where a direct relation is present according to equations 7, 14, and 17, there is an increase in the values of the gain bandwidth Δv_{gain} and the number of n_{mode} as a result of increasing energy spread $\epsilon_s$values. The effect is more evident at high values of electron wavelengthλ_u.

Figure 5: The effect of changing the energy spread $\in_s$ on the small signal gain g_0, transmittance T, pulse duration τ, gain bandwidth Δv_{gain} and number of n_{mode}.

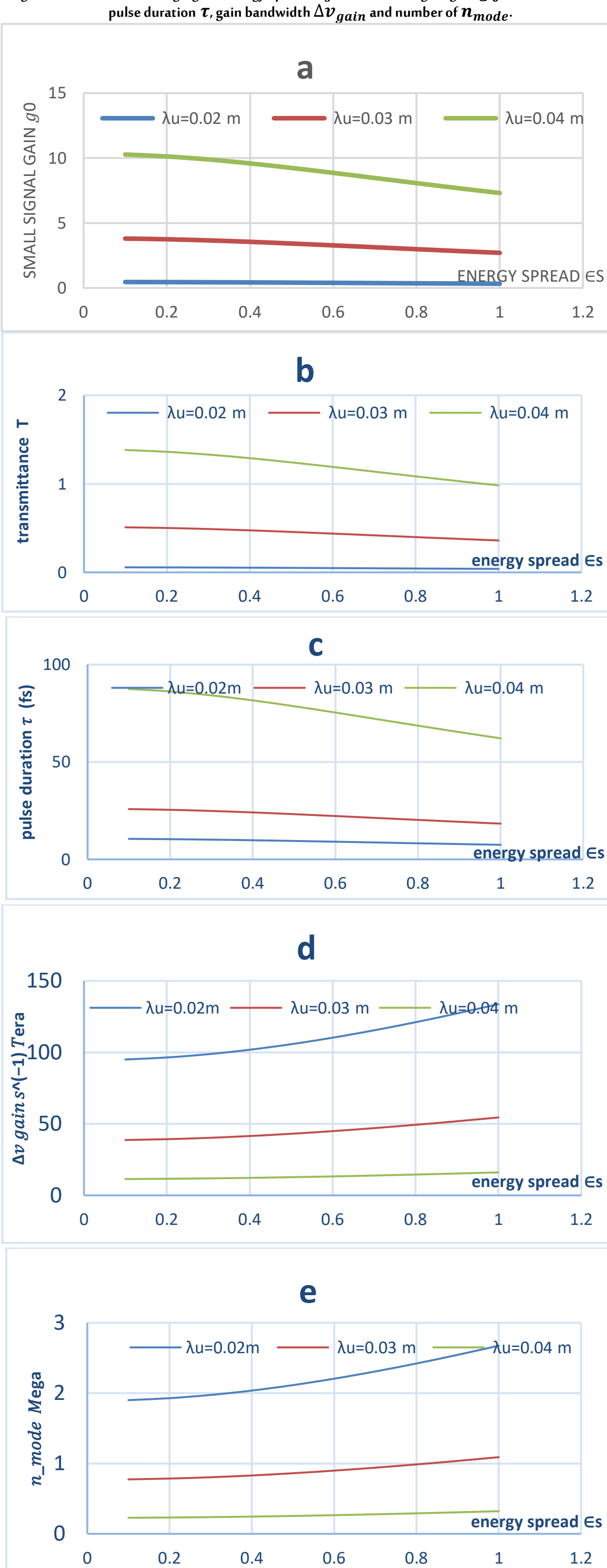

Table 5: The simulation results for the relation between the length of an ideal Fabry–Perot cavity L vs. the bunching frequency v and the round-trip time.

Table5: The results of simulation for L vs. v and τr.

L	v(MHz)	$\tau_r(ns)$
1	150	6.66
2	75	13.3
3	50	20
4	37.5	26.66
5	30	33.33
6	25	40
7	21.4	46.66
8	18.7	53.33
9	16.6	60
10	15	66.66

Figure 6-a and Figure 6-b show the effect of changing the length of the resonator L on the bunching frequency v and the round-trip timeτ_r. There is an inverse relation with the bunching frequency v and a direct relation with the round trip-time τ_r according to equation 18. In a Fabry–Perot resonator, the condition of resonance requires a match between v and FSR, so the corresponding parameters were determined for τ_r and gain switching. The round-trip time $\tau_r = 20ns$ was chosen (as shown in Table 2), corresponding to the length $L = 3\ m$ used in the simulation.

Figure 6: shows the effect of changing length of resonator L on both the bunching frequency and the round-trip timeτ_r.

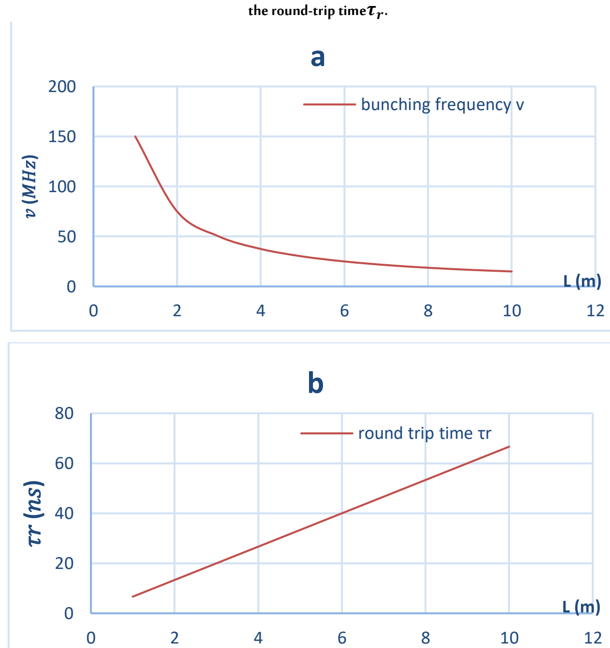

4. Conclusions

From the analysis of the obtained simulation results, it can be concluded that the small signal gain g_0 is affected by the energy spread $\in_s$; thus, the set of parameters of the laser resonator SR-FEL can be controlled. The main goal of this paper was to generate short pulses between 7.4–87.4 fs with the Fabry–Perot resonator using the fewest modes (n_{mode}) possible because there is an increase in the values of the gain bandwidth Δv_{gain} and the number of n_{mode} as a result of increasing the energy spread.

Biographies

Thair Abdulkareem Khalil Al-Aish

Department of Physics, College of Education for Pure Sciences, Ibn Al-Haitham, University of Baghdad, Baghdad, Iraq, 009647801693969, thair.ak.i@ihcoedu.uobaghdad.edu.iq

Dr. Al-Aish is a university of Baghdad graduate and an Iraqi assistant professor. He has published 20 Scopus-indexed articles with global publishers. Many countries cite his work. He teaches a laser subject at the college for bachelor's, master's, and doctoral students. He supervises masters and doctoral students. He is a supervisor at the optics and laser lab, computer lab, and information and media unit manager. He has participated in conferences in Iraq, Greece, Lebanon, and France. ORCID: 0000-0003-2479-5840

Hanady Amjed Kamil

Directorate of Education of First Karkh, Ministry of Education, Baghdad, Iraq, 009647813038914, hanadyamjedkamil@gmail.com

Kamil is a university of Baghdad graduate and an Iraqi assistant lecturer. She obtained a master's degree in Laser Physics. She has published 7 Scopus-indexed articles with global publishers. Many countries cite her work. She is interested in researching the interaction of a laser beam with matter in various applications. She teaches physics at the Directorate of Education of First Karkh, Ministry of Education, Baghdad, Iraq. She has participated in conferences in Iraq, Greece, Lebanon, and France. ORCID: 0000-0003-4485-1475.

References

Al-Aish, T.A. and Jawad, R.L. (2017). Design and simulate a new defense system of free electron laser DSFEL. *Engineering and Technology Journal*, **35**(2B), 166–72.

Al-Aish, T.A.K. (2017). Analysis and study of the effect of atmospheric turbulence on laser weapon in Iraq. *Baghdad Science Journal*, **14**(2), 426–37. DOI: 10.21123/bsj.2017.14.2.0427.

Al-Aish, T.A.K. and Kamil, H.A. (2022). Simulation and analysis the effect of the Lorentz force in a free electron laser. *Ibn AL-Haitham Journal for Pure and Applied Sciences*, **35**(2), 7–16. DOI:10.30526/35.2.2775.

Al-Aish, T.A.K., Jawad, R.L. and Kamil, H.A. (2019). Design and simulation a high-energy free electron laser HEFEL. In: *AIP Conference Proceedings*, AIP Publishing LLC, Beirut, Lebanon, 10–12/04/2019. DOI: 10.1063/1.5116995.

Ali, M.A., Al-Aish, T.A.K. and Kamil, H.A. (a2022). Analyzing and simulating the mechanism of laser medical therapy. In: *AIP Conference Proceedings*, AIP Publishing LLC, Athens, Greece, 28–30/05/2021. DOI: 10.1063/5.0092605.

Ali, M.A., Al-Aish, T.A.K. and Kamil, H.A. (b2022). A simulation breakdown the blood clot using a free electron laser system. In: *AIP Conference Proceedings*, AIP Publishing LLC, Athens, Greece, 28–30/05/2021. DOI: 10.1063/5.0092607.

Benson, S.V., Douglas, D., Neil, G.R. and Shinn, M.D. (2011). The Jefferson Lab free electron laser program. In: *Journal of Physics: Conference Series*, IOP Publishing. Virginia, USA, 8–11/06/2011. DOI 10.1088/1742-6596/299/1/012014.

Dattoli, G., Renieri, A. and Torre, A. (1993). *Lectures on the Free Electron Laser Theory and Related Topics*. London, UK: World Scientific.

Davis, C.C. (1996). *Lasers and electro-optics: Fundamentals and Engineering*. New York, USA: Cambridge University Press.

Dhedan, Z.A., Al-Aish, T.A.K. and Kamil, H.A. (2022). Design and simulation of a new system for producing laser beams without resonator "NSPLBR". In: *AIP Conference Proceedings*, AIP Publishing LLC, Athens, Greece, 28–30/05/2021. DOI: 10.1063/5.0092603.

Haarlammert, T. and Zacharias, H. (2009). Application of high harmonic radiation in surface science. *Current Opinion in Solid State and Materials Science*, **13**(1-2), 13–27.

Hannon, F.E. (2008). *A High Average-Current Electron Source for the Jefferson Laboratory Free Electron Laser*. PhD Thesis, Lancaster University, Lancaster, United Kingdom.

Kamil, H.A. and Al-Aish, T.A.K. (2022). Determine the hazard level and biological effects for visible laser pointers. In: *AIP Conference Proceedings*, AIP Publishing LLC, Athens, Greece, 28–30/05/2021. DOI: 10.1063/5.0092595.

Kamil, H.A., Ahmed, M.S. and Al-Aish, T.A.K. (2019). Rain formation by free electron laser pulse system FELPS. In: *AIP Conference Proceedings*, AIP Publishing LLC, Beirut, Lebanon, 10–12/04/2019. DOI: 10.1063/1.5138570.

Kawamura, Y., Toyoda, K. and Kawai, M. (1987). Observation of periodical short pulse trains in free-electron laser oscillations. *Applied Physics Letters*, **51**(11), 795–7.

Kryukov, P. and Letokhov, V. (1972). Fluctuation mechanism of ultrashort pulse generation by laser with saturable absorber. *IEEE Journal of Quantum Electronics*, **8**(10), 766–82.

Mahmood, H.K. and Al-Aish, T.A.K. (2020). Design and stimulated the detectors of high-power lasers DHPL. In: *AIP Conference Proceedings*, AIP Publishing LLC, Athens, Greece, 28–30/05/2021. DOI: 10.1063/5.0092603.

Mehravaran, H., Parvin, P. and Dorranian, D. (2010). Changeover in the molecular and atomic fluorine laser transitions. *Applied optics*, **49**(15), 2741–8.

Moulton, P.F. (1986). Spectroscopic and laser characteristics of Ti:Al_2O_3. *JOSA B*, **3**(1), 125–33.

Parvin, P., Mortazavi, S.Z. and Korabaslo, M.N. (2012). Possibility for mode-locked operation of a femtosecond UV storage ring free-electron laser using a low-loss Fabry–Perot resonator. *Optics and Laser Technology*, **44**(7), 2161–7.

Parvin, P., Zaeferani, M.S., Mirabbaszadeh, K. and Sadighi, R. (1997). Measurement of the small-signal gain and saturation intensity of a XeF discharge laser. *Applied optics*, **36**(6), 1139–42.

Penzkofer, A. (1988). Passive Q-switching and mode-locking for the generation of nanosecond to femtosecond pulses. *Applied physics B*, **46**(1), 43–60.

Varro, S. (2012). *Free Electron Lasers*. Rijeka, Croatia: BoD–Books on Demand.

Wieduwilt, T., Dellith, J., Talkenberg, F., Bartelt, H. and Schmidt, M.A. (2014). Reflectivity enhanced refractive index sensor based on a fiber-integrated Fabry-Perot microresonator. *Optics express*, **22**(21), 25333–46.

Zegadi, R., Lorrain, N., Meziani, S., Dumeige, Y., Bodiou, L., Guendouz, M. and Charrier, J. (2022). Theoretical demonstration of the interest of using porous germanium to fabricate multilayer vertical optical structures for the detection of SF6 gas in the mid-infrared. *Sensors*, **22**(3), 844.